

Mechanisms of Nickel Sorption on Pyrophyllite: Macroscopic and Microscopic Approaches

André M. Scheidegger,* Mark Fendorf, and Donald L. Sparks

ABSTRACT

Retention of heavy metal ions on soil mineral surfaces is a crucial process for maintaining environmental quality. A thorough understanding of the sorption mechanisms of heavy metals on soil mineral surfaces is therefore of fundamental importance. This study examined Ni(II) sorption mechanisms on pyrophyllite. The removal of Ni from solution was studied as a function of pH (pH = 5–8.5), initial Ni concentration (1×10^{-4} to 1×10^{-2} M), and ionic strength (0.01–1 M). The data suggest that Ni sorption behavior can be divided into two distinct pH regions. In the lower pH region (i.e., pH < 7), relative Ni sorption increased with decreasing ionic strength and initial Ni concentration. The adsorption maximum at pH = 6 was significantly higher than the cation-exchange capacity (CEC) at the same pH. Based on these findings, we propose that both specific and nonspecific adsorption are involved. In the higher pH region (pH > 7), nickel sorption becomes slow and does not seem to be affected by the ionic strength and the initial Ni concentration. We employed high-resolution transmission electron microscopy (HRTEM) to ascertain whether any alteration in the surface structure of pyrophyllite could be detected after reaction with Ni at pH > 7. Surface deposits, not present on untreated samples, were found. At low Ni sorption densities, surface precipitation seems to occur preferentially along the edges of the particles. Based on the HRTEM findings, and on results from a previous x-ray absorption fine structure spectroscopy (XAFS) study, we hypothesize that the formation of a mixed Ni–Al hydroxide phase on the pyrophyllite surface is responsible for the sorption behavior above pH 7.

A.M. Scheidegger and D.L. Sparks, Dep. of Plant and Soil Sciences, Univ. of Delaware, Newark, DE 19717-1303; and M. Fendorf, National Center for Electron Microscopy, Lawrence Berkeley National Lab., Berkeley, CA 94720. Received 6 Nov. 1995. *Corresponding author (scheideg@brahms.udel.edu).

Published in Soil Sci. Soc. Am. J. 60:1763–1772 (1996).

SORPTION REACTIONS at solid–water interfaces decrease solute mobility and often control the fate, bioavailability, and transport of trace metal ions such as Zn, Cd, Pb, Ni, and Cu in aquatic and soil environments. Correctly determining the sorption mechanisms of metals on clay and other mineral surfaces is therefore of great importance for understanding the fate of such pollutants in contaminated soils and sediments, and will facilitate successful environmental remediation procedures.

The significance of ion exchange reactions was recognized as important in nutrient dynamics in soils long before structure and chemical composition of clays were completely known (McBride, 1994, p. 63–120). The present understanding of ion exchange reactions involving metal cations in soils is largely based on experiments with Na⁺-saturated sorbents such as the Wyoming, Camp Berteau, and Chambers montmorillonites (Peigneur et al., 1975; Inskeep and Baham, 1983; Fletcher and Sposito, 1989). These studies have shown that Na⁺–Me²⁺ exchange reactions on montmorillonite are relatively insensitive to pH at low pH values, i.e., pH < 6 (Peigneur et al., 1975; Zachara et al., 1993). However, at higher pH values, i.e., pH > 6, adsorption of metal cations on layer silicates increases with increasing pH (Peigneur et al., 1975; Inskeep and Baham, 1983; Puls and Bohn, 1988; Schulthess and Huang, 1990; Cowan et al., 1992; Zachara et al., 1994). In addition, at elevated pH values,

Abbreviations: CEC, cation-exchange capacity; TEM, transmission electron microscopy; HRTEM, high-resolution transmission electron microscopy; XAFS, x-ray absorption fine structure spectroscopy; ICP, inductively coupled plasma emission.

the removal of metal ions from solution by clay surfaces is accompanied by a release of H ions (Schindler et al., 1987). Adsorption of metals generally becomes more specific as the solution pH increases; i.e., formation of inner sphere complexes is favored at elevated pH (Schindler et al., 1987). Based on sorption experiments and potentiometric titrations, the pH-dependent metal sorption on clay surfaces is usually modeled assuming two classes of sites: (i) ion exchange or nonspecific adsorption sites that exchange background electrolyte cations with weakly bound, hydrated metal ions (outer sphere complexes) and (ii) specific adsorption at amphoteric surface hydroxyl sites (Al-OH, Si-OH) in which surface sites hydrolyze; metal ions then bond directly to surface O or OH groups and are not easily displaced by electrolyte ions (inner sphere complexes) (Farrar et al., 1980; Sposito, 1984, p. 234; Schindler et al., 1987; Zachara et al., 1988; Cowan et al., 1992; Singh and Mattigold, 1992; Wieland and Stumm, 1992; Zachara et al., 1994). Different surface complexation models have reproduced experimental data equally well, even when the models have differed significantly in the number and types of reactions included, in the surface adsorption sites chosen to bind cations, in whether complexes bind as inner or outer sphere complexes, and in the values of the stability constants used to describe sorption reactions (O'Day et al., 1994b).

Recent studies using surface spectroscopic and microscopic techniques such as XAFS, electron spin resonance spectroscopy, x-ray photoelectron spectroscopy, Auger electron spectroscopy, scanning electron microscopy, atomic force microscopy, and TEM have shown that the adsorption of heavy metals on clay and oxide surfaces results in the formation of multinuclear or polynuclear surface complexes much more frequently than previously thought (Fendorf et al., 1992a,b, 1993, 1994; Charlet and Manceau, 1993; Fendorf and Sparks, 1994; Junta and Hochella, 1994; O'Day et al., 1994a,b; Wersin et al., 1994; Fendorf and Fendorf, 1996). Multinuclear metal hydroxides of Pb, Co, Cu, and Cr(III) on oxides and aluminosilicates have been observed with XAFS (Charlet and Manceau, 1993; Fendorf et al., 1994; O'Day et al., 1994a) and electron spin resonance spectroscopy (McBride et al., 1984; Bleam and McBride, 1986; Wersin et al., 1994). Such surface complexes, or surface precipitates, have been observed at surface metal loadings far below a theoretical monolayer coverage, and in a pH range well below the pH where the formation of metal hydroxide precipitates would be expected according to the thermodynamic solubility product (speciation based on crystalline metal hydroxide; Charlet and Manceau, 1993; Fendorf et al., 1994; O'Day et al., 1994a; Fendorf and Fendorf, 1996).

This study examined Ni(II) sorption mechanisms on pyrophyllite. The Ni²⁺ cation, like many other metal ions (e.g., Co²⁺, Cd²⁺, Pb²⁺, Mn²⁺, Cu²⁺, Zn²⁺, and Cr³⁺), has a tendency to be adsorbed specifically on clay and oxide surfaces and to hydrolyze within common environmental pH ranges (pH 3–9) (Puls and Bohn, 1988; Schulthess and Huang, 1990). The removal of Ni from solution was studied as a function of pH, initial

Ni concentration, and ionic strength. X-ray absorption fine structure spectroscopy was previously used to determine the local structural environment of Ni(II) sorbed onto pyrophyllite (Scheidegger et al., 1996). The XAFS data revealed the formation of surface precipitates at low surface loadings. The presence of a mixed Ni-Al hydroxide phase was proposed. In this work TEM was employed to ascertain whether any alteration in the surface structure of pyrophyllite could be detected after reaction with Ni.

Pyrophyllite was chosen for these experiments in order to study the effect of edge surface properties of clays on Ni sorption. Pyrophyllite, in contrast to montmorillonite and illite, shows little deviation from the ideal chemical formula [Al₂Si₄O₁₀(OH)₂] of 2:1 clay minerals. Its dioctahedral structure consists of essentially neutral tetrahedral-octahedral-tetrahedral layers. Hence, the complexity associated with the permanent charge of planar clay surfaces can be avoided and sorption of ions on pyrophyllite can be ascribed to only edge surface sites (Keren and Sparks, 1994; Keren et al., 1994).

MATERIALS AND METHODS

Materials

The pyrophyllite used in this study originated from Robins, NC. It was ground in a mortar to a size fraction of <125 μm and transferred to a porcelain ball mill, which was one-third filled with hard, ball-shaped, wear-resistant media (Zirconia), and then dry ground for 30 h. The <2-μm clay size fraction was obtained by centrifuging and decanting. The pyrophyllite was saturated with Na by washing three times with 0.5 M NaNO₃, then resuspended with distilled water and centrifuged. The clear supernatant was discarded and excess salts removed by dialysis until the electrical conductivity of the equilibrium solution was <10 μS cm⁻¹. Thereafter, the white clay material was freeze-dried.

The pyrophyllite was characterized by x-ray diffraction using a Philips (Eindhoven, the Netherlands) PW1729 diffractometer and by diffuse reflectance infrared Fourier transform spectroscopy using a Perkin-Elmer (Buckinghamshire, England) 1720X spectrometer. The infrared spectra showed only the characteristic peaks for pyrophyllite (Russell et al., 1970), while x-ray diffraction spectra suggested the presence of a small amount of quartz (<5%) in addition to pyrophyllite. No porcelain or zirconia residue from the grinding process was detected. The specific surface area of pyrophyllite was 43.7 ± 0.3 m²/g, as determined by the BET method using N₂ adsorption (Keren et al., 1994). The CEC of the clay (0.041 mol_e/kg, pH 6) was determined by Na-NH₄ exchange experiments.

Batch Studies

Nickel sorption envelopes on pyrophyllite were measured using a batch technique designed to maintain constant pH (pH-stat, Radiometer, Copenhagen, Denmark) and temperature (298 K) and to eliminate CO₂ by purging with N₂. The pyrophyllite was hydrated for 24 h prior to reaction with Ni. After hydration, a desired amount of Ni from a 0.01 or 0.1 M Ni(NO₃)₂ stock solution (pH ≈ 6) was dispensed, the ionic strength adjusted, and the mixture brought to a solid/liquid ratio of 10 g/L. The reaction mixture was then titrated with 0.01 or 0.1 M NaOH in small pH increments from pH ≈ 5 to 8.5 using the pH-stat apparatus. The reaction time between

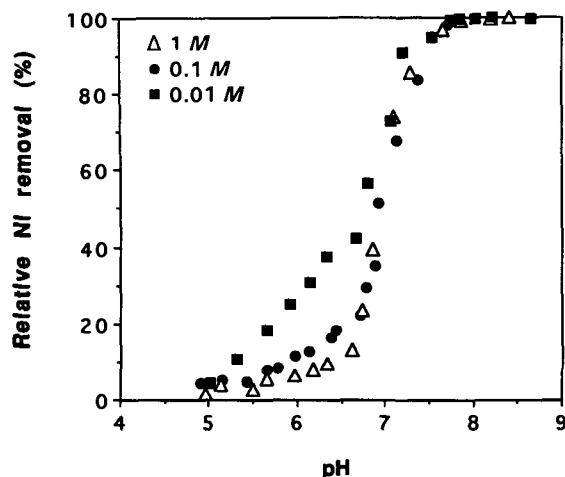


Fig. 1. Adsorption of Ni on pyrophyllite as a function of pH (Ni adsorption envelope): The relative Ni removal (in percentage) from a 10^{-3} M Ni solution is represented for three different ionic strengths. The solid/liquid ratio was 10 g/L.

each small pH increment varied between 2 and 4 h in the lower pH region ($\text{pH} < 6.5$) and 12 to 24 h in the higher pH region ($\text{pH} > 6.5$). The electrode was recalibrated every 24 h. Samples were collected and passed through a $0.22\text{-}\mu\text{m}$ membrane filter. The clear solutions were analyzed for Ni by ICP spectrometry.

A Ni sorption isotherm on pyrophyllite was determined similarly. After hydration of the clay, the ionic strength (0.1 M NaNO_3) and the reaction pH ($\text{pH} 6$, 0.1 M NaOH) were adjusted and the mixture brought to a solid/liquid ratio of 20 g/L. The desired amount of Ni was then dispensed and the pH was automatically held constant ($\text{pH} 6$, 0.1 M NaOH). After a reaction time of 2 to 4 h, a small sample was removed and filtered for ICP analysis. An additional Ni increment was then added to the main reaction vessel. The above procedure was repeated for each sample.

Electron Microscopy

High-resolution and conventional TEM were performed using a JEOL (Tokyo, Japan) JEM 200CX and a Topcon 002B, both operating at 200kV. Energy dispersive x-ray spectroscopy was performed using a Philips (Eindhoven, the Netherlands) EM400 operating at 100kV, with a probe size of approximately 100 nm. The materials for the TEM study were reacted by hydrating the clay, adjusting the ionic strength (0.1 M NaNO_3), the reaction pH ($\text{pH} 7.5$, 0.1 M NaOH), and the solid/liquid ratio (10 g/L), then dispensing Ni in stepwise additions within ≈ 15 min in order to avoid the formation of Ni precipitates due to local oversaturation of the suspension. The pH was automatically held constant ($\text{pH} 7.5$) and the mixtures were allowed to equilibrate for at least 3 d so that the concentration of Ni remaining in solution was small. Specimens were prepared for TEM examination by transferring a few drops of a suspension onto a copper mesh grid with holey carbon support film (see, for example, Fendorf et al., 1995). The grid was gently but thoroughly rinsed with deionized water once the particles had been deposited, i.e., before the solution had a chance to begin to dry.

RESULTS AND DISCUSSION

Nickel sorption on pyrophyllite was studied at various metal concentrations and ionic strengths (I). Figure 1

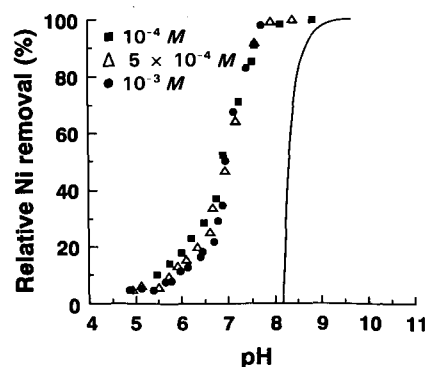


Fig. 2. Nickel adsorption envelopes: The relative Ni removal from solution (in percentage) at a constant ionic strength ($I = 0.1$ M) is shown for three different initial Ni concentrations. The solid/liquid ratio was 10 g/L. The solid line represents the expected formation of crystalline Ni hydroxide precipitates in homogeneous solution according to the thermodynamic solubility product when $[\text{Ni}] = 10^{-3}$ M and $I = 0.1$ M.

shows the relative Ni removal from solution ($[\text{Ni}]$ initial = 10^{-3} M) as a function of the pH for three different ionic strengths (0.01, 0.1, and 1 M). The results from the sorption envelope experiments reveal that the adsorption behavior can be divided into two pH regions. In the lower pH region, i.e., $\text{pH} < 7$, the relative Ni removal from solution increased with decreasing ionic strength, while in the higher pH region ($\text{pH} > 7$), Ni sorption seems not to be affected by ionic strength.

Similar observations were found studying the relative Ni sorption from solution as a function of the pH for three different initial Ni concentrations (see Fig. 2). In a pH region below approximately $\text{pH} 7$, the relative Ni removal increased with decreasing initial Ni concentration. On the other hand, in the pH region where the relative Ni removal from solution increased sharply up

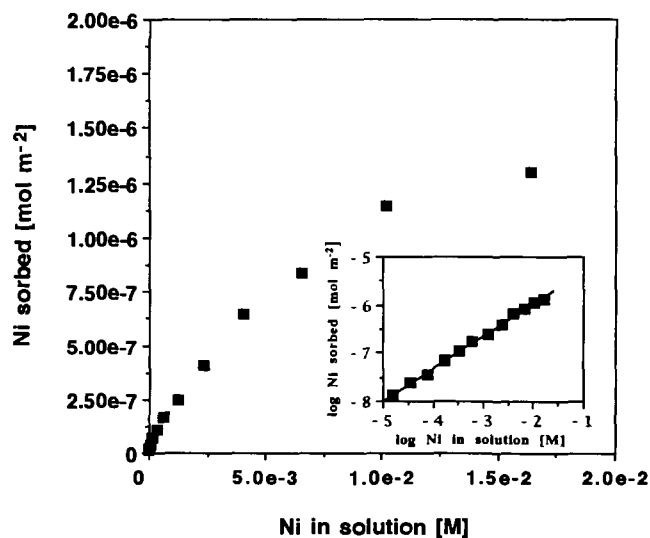


Fig. 3. Nickel adsorption isotherm at $\text{pH} 6$, a constant ionic strength of 0.1 M (NaNO_3), and a solid/liquid ratio of 20 g/L: The amount of Ni adsorbed (mol/m^2) is shown as a function of the nickel concentration in solution (M). The inset represents the sorption data plotted on a logarithmic scale. The data were linearly fitted to determine the Freundlich exponent α of the adsorption isotherms ($\alpha = 0.67$).

to 100%, the sorption data didn't exhibit any dependence on initial metal concentrations. To demonstrate that the reaction conditions were undersaturated with respect to crystalline $\text{Ni}(\text{OH})_2(\text{s})$, the pH where the formation of Ni-OH precipitates in homogeneous solution would be expected is shown for comparison (solid line in Fig. 2; speciation for $[\text{Ni}] = 10^{-3} \text{ M}$ and $I = 0.1 \text{ M}$). Nickel speciation was performed using a chemical equilibrium speciation program based on a thermodynamic database (Environmental Simulation Program, OLI Systems, Morristown, NJ). Data reported by Glushko et al. (1972), Gurvich et al. (1993), Shock and Helgeson (1988), and Sverjensky (1987; personal communication, 1988) were considered. The speciation reveals that Ni(II) is predominately present as $\text{Ni}^{2+}(\text{aq})$ ($\approx 90\%$) and to a minor extent as $\text{NiNO}_3^-(\text{aq})$ ($\approx 9\%$; Scheidegger et al., 1996). The concentrations of hydrolysis products such as $\text{Ni}(\text{OH})^+$ and $\text{Ni}(\text{OH})_2^0$ are extremely low. Further details on the speciation are given elsewhere (Scheidegger et al., 1996).

Figure 3 shows a Ni adsorption isotherm on pyrophyllite at pH 6 and a constant ionic strength of 0.1 M NaNO_3 . The isotherm is strongly convex. The data set is fit well by a Freundlich isotherm, $y = Kx^\alpha$, where y is the amount of Ni adsorbed (mol/m^2), x is the Ni concentration in solution (M), and α denotes the Freund-

lich exponent. The inset illustrates a logarithmic plot of the sorption data in comparison with the fit (Fig. 3). The slope of the solid line represents the Freundlich exponent, α , which was found to be 0.67. Such a small Freundlich exponent demonstrates that Ni sorption on pyrophyllite at pH 6 is highly nonlinear. Because of this nonlinearity, we simply considered the highest observed Ni adsorption density ($1.3 \mu\text{mol m}^{-2}$) for making a rough estimate of maximal Ni adsorption at pH 6. This value, used later for a comparison, slightly underestimates the adsorption maximum (if such exists) under the reaction conditions employed.

The results from the Ni sorption isotherm experiment coincide with results from the adsorption envelope experiments. If the sorption data from Fig. 2 at pH ≈ 6 ($[\text{Ni}]_{\text{initial}} = 1 \times 10^{-4}$, 5×10^{-4} , and 10^{-3} M) are incorporated in Fig. 3, they agree well with the adsorption isotherm. Furthermore, the results from the Ni adsorption envelope experiments suggest that the Ni sorption behavior on pyrophyllite changed significantly when the reaction pH was increased from pH 6 to 7.5 (Fig. 1 and 2). Several studies of divalent cation (Me^{2+}) sorption on kaolinite support our findings (Schindler et al., 1987; Cowan et al., 1992; O'Day et al., 1994b; Zachara et al., 1994). These studies showed that (i) relative metal



Fig. 4. Low-magnification transmission electron microscope image of unreacted pyrophyllite, showing plate- and needle-like structures characteristic of this material. Note the absence of any visible surface deposits.

removal from solution is low at low pH and rises rapidly in a narrow pH range, and (ii) metal removal from solution is reduced by increasing ionic strength at low pH while it is insensitive to changes in electrolyte concentrations at high pH.

Traditionally, the ionic strength dependence of metal ion removal from solution by soil minerals was used to distinguish between nonspecific and specific adsorption. Outer sphere complexes involve only electrostatic interactions and are strongly affected by the ionic strength of the aqueous phase, while inner sphere complexes involve much stronger covalent or ionic binding and are only weakly affected by the ionic strength (Sparks, 1995, p. 99–139). Our sorption data showed a pronounced ionic strength dependence in a low pH region (pH < 7). Thus, one could be tempted to explain Ni sorption on pyrophyllite at low pH by nonspecific adsorption alone. We tried to further address the question whether Ni is adsorbed specifically or nonspecifically to the pyrophyllite surface by comparing the CEC of pyrophyllite to the charge density of the clay and to the adsorption maximum for Ni. The CEC of pyrophyllite at pH 6 ($\approx 1 \times 10^{-6} \mu\text{mol}_c \text{ m}^{-2}$; see above) agrees well with the charge density of the clay at pH 6 as determined by acid–base titration ($1.2 \times 10^{-6} \mu\text{mol}_c \text{ m}^{-2}$; $I = 0.1 \text{ M}$

NaNO_3 ; R. Keren, 1995, personal communication). This result is not surprising since pyrophyllite has almost no permanent charge and the entire negative charge is associated with deprotonated edge surface sites (Keren and Sparks, 1995). To compare the CEC of pyrophyllite at pH 6 to the Ni adsorption maximum at pH 6 (Fig. 3), it was necessary to express the amount of sorbed Ni in $\mu\text{mol}_c \text{ m}^{-2}$, since Ni is a divalent ion. The calculated value ($2.6 \times 10^{-6} \mu\text{mol}_c \text{ m}^{-2}$) is distinctly higher than the CEC ($1 \times 10^{-6} \mu\text{mol}_c \text{ m}^{-2}$), suggesting that specific adsorption is involved, even when the reaction is carried out at a relatively low pH value (pH 6). It is important to note that outer and inner sphere complexation can, and apparently do in our case, occur simultaneously (Sparks, 1995, p. 99–139).

In the higher pH region, Ni sorption data showed no dependence on the initial Ni concentration or on ionic strength. Furthermore, while the kinetics of Ni sorption at pH 6.0 was found to be fast (equilibrium reached within minutes) and reversible (Scheidegger, 1995, unpublished data), Ni sorption was much slower at pH 7.5. In spite of the fact that a reaction time of 12 to 24 h was chosen between each small pH increment, sorption data in this pH region may not be necessarily indicative of sorption at equilibrium. Relative Ni removal from solution is

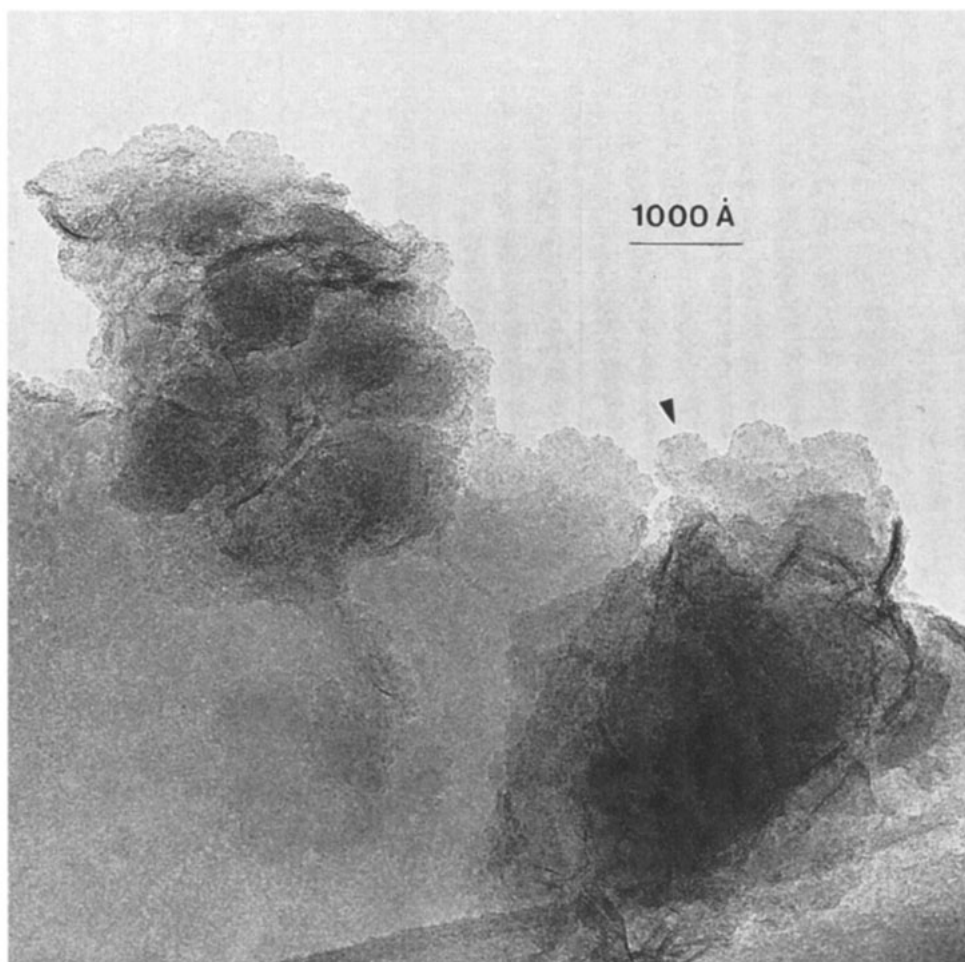


Fig. 5. Low-magnification transmission electron microscope image of a heavily Ni-treated pyrophyllite surface (Ni sorption density = $26.5 \mu\text{mol}/\text{m}^2$). A new surface phase can now clearly be seen (indicated by arrow) along the particle edges.

strongly influenced by the reaction time and therefore no adsorption isotherm experiment was performed at pH 7.5. A previous kinetic study on the removal of Ni by pyrophyllite from a solution with an initial Ni concentration of 10^{-3} M showed that at pH 7.5, 90% of the Ni was removed within 24 h, and 97% within 3 d (Scheidegger and Sparks, 1996). The slow sorption kinetics was attributed to nucleation processes on the pyrophyllite surface (surface precipitation). According to the definition of Sposito (1986), a precipitation mechanism may be initiated by either homogenous or heterogenous nucleation, may involve the formation of a solid mixture either by inclusion or by coprecipitation, or may take place on the surface of a preexisting solid phase. In the last case, the process is called *surface precipitation*. A kinetic study of Mn(II) sorption on FeCO_3 revealed similar findings (Wersin et al., 1989). At high Mn(II) concentrations, the sorption decreased considerably after a rapid initial reaction, and required several days to reach equilibrium. Electron spin resonance spectroscopy provided evidence that the slow sorption kinetics were the result of the precipitation of a mixed MnCO_3 and FeCO_3 solid phase.

In this study, conventional, high-resolution (HRTEM)

and analytical TEM techniques proved useful in ascertaining whether any alteration in the surface structure of pyrophyllite could be detected after reaction with Ni at pH 7.5. The technique was previously used to determine surface alterations on oxide surfaces after reaction with hydrolyzable metal ions (Fendorf et al., 1992a,b, 1993; Fendorf and Fendorf, 1996).

Zelazny and White (1989) reported that pyrophyllite particles can be identified optically by the lath-like plates, which have distinct angular edges or can extend to blades or needles. Another common pyrophyllite morphology is radial aggregates (Hurlbut, 1971). Figure 4, a TEM image of untreated pyrophyllite, reveals the presence of all these features. After the reaction with Ni ($[\text{Ni}]_{\text{initial}} = 1.1 \times 10^{-2}$ M; pH 7.5), a distinct change in the surface structure can be observed at a similar magnification (see Fig. 5). While in some parts of the image plate and needle-like structures are still apparent, there are unmistakable rough, scalloped, "cauliflower-like" deposits along the particle edge (see arrow in Fig. 5). These features, not seen in the untreated sample, clearly demonstrate the presence of a surface precipitate. The surface deposits in this heavily Ni-treated pyrophyllite sample

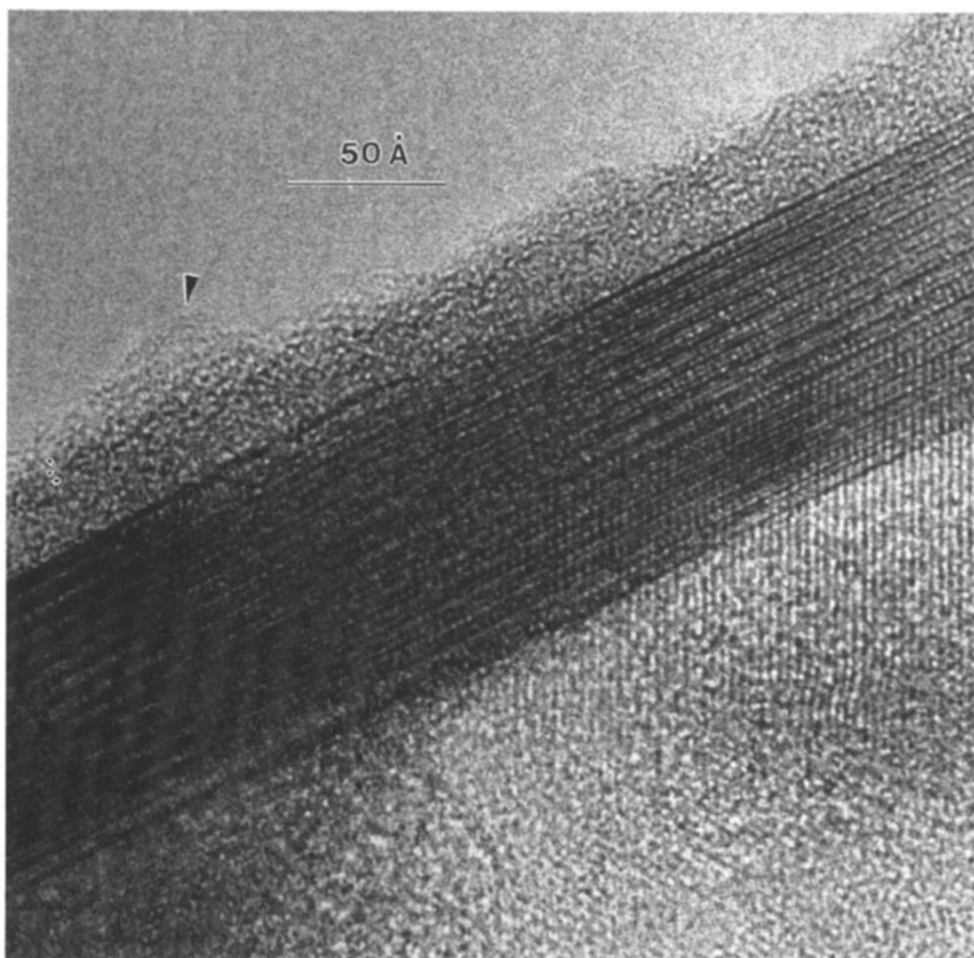


Fig. 6. High-resolution transmission electron microscope image of a Ni-treated pyrophyllite surface at low Ni sorption density ($0.46 \mu\text{mol}/\text{m}^2$); note the scale change from Fig. 4 and 5. A small cluster-type structure can be discerned on the surface, which illustrates an early stage of surface precipitation (see arrow).

(Ni sorption density = $26.5 \mu\text{mol}/\text{m}^2$) appear to be slightly greenish.

Figure 6 shows a HRTEM image of a pyrophyllite sample with approximately 50 times lower Ni sorption density ($0.46 \mu\text{mol}/\text{m}^2$). Lattice fringes characteristic of pyrophyllite can be seen in this image, demonstrating a high degree of crystallinity. However, on close inspection, a structural alteration can again be observed along the particle edge (see arrow in Fig. 6), with deposits similar in form to those in Fig. 5, but much less extensive. We attribute this appearance to an early stage of surface precipitation. Findings from a previous XAFS study on Ni sorption on pyrophyllite at pH 7.5 (Scheidegger et al., 1996) support our suggestion. Changes in the XAFS spectra with increasing Ni sorption were examined and the data suggested the presence of surface precipitates at Ni sorption densities as low as $0.49 \mu\text{mol}/\text{m}^2$.

Figure 7 presents a HRTEM image of a sample with a significantly higher Ni sorption density ($1.44 \mu\text{mol}/\text{m}^2$) at high magnification. The image illustrates how the surface deposits grow. Rather than a homogenous precipitate, we observe clustered structures that protrude from the surface. Their width varies considerably, ranging from a few up to 30 nm. Surface precipitation seems to occur preferentially along the edges of the particle. The

bottom and top faces of the particle have not noticeably changed upon Ni sorption; the lattice fringes of pyrophyllite are still clearly visible. This finding tends to support the current understanding that edge surface sites are of great importance for metal removal from solution by clay mineral surfaces (Schindler et al., 1987; Zachara et al., 1993; Keren and Sparks, 1994; Keren et al., 1994; O'Day et al., 1994b). However, Fig. 8a demonstrates that surface precipitation is not entirely restricted to the particle edges when the Ni concentration is near saturation. In this TEM image of a heavily Ni-treated pyrophyllite sample (Ni sorption density = $26.5 \mu\text{mol}/\text{m}^2$) there are changes in contrast that indicate the presence of similar deposits on the top and bottom faces of the particle (see arrow). This finding is in agreement with energy dispersive x-ray spectroscopy analysis of the sample. The height of the Ni peak in the x-ray spectrum remained almost constant as the electron beam was moved from an edge to the interior of a particle, indicating that Ni is fairly uniformly distributed over all particle surfaces. Here, "uniformity" is on a scale determined by the diameter of the electron beam used as a probe, and in our work this diameter was approximately 100 nm. Figure 8b shows a similar TEM image of a sample with lower Ni sorption density ($0.46 \mu\text{mol}/\text{m}^2$). The

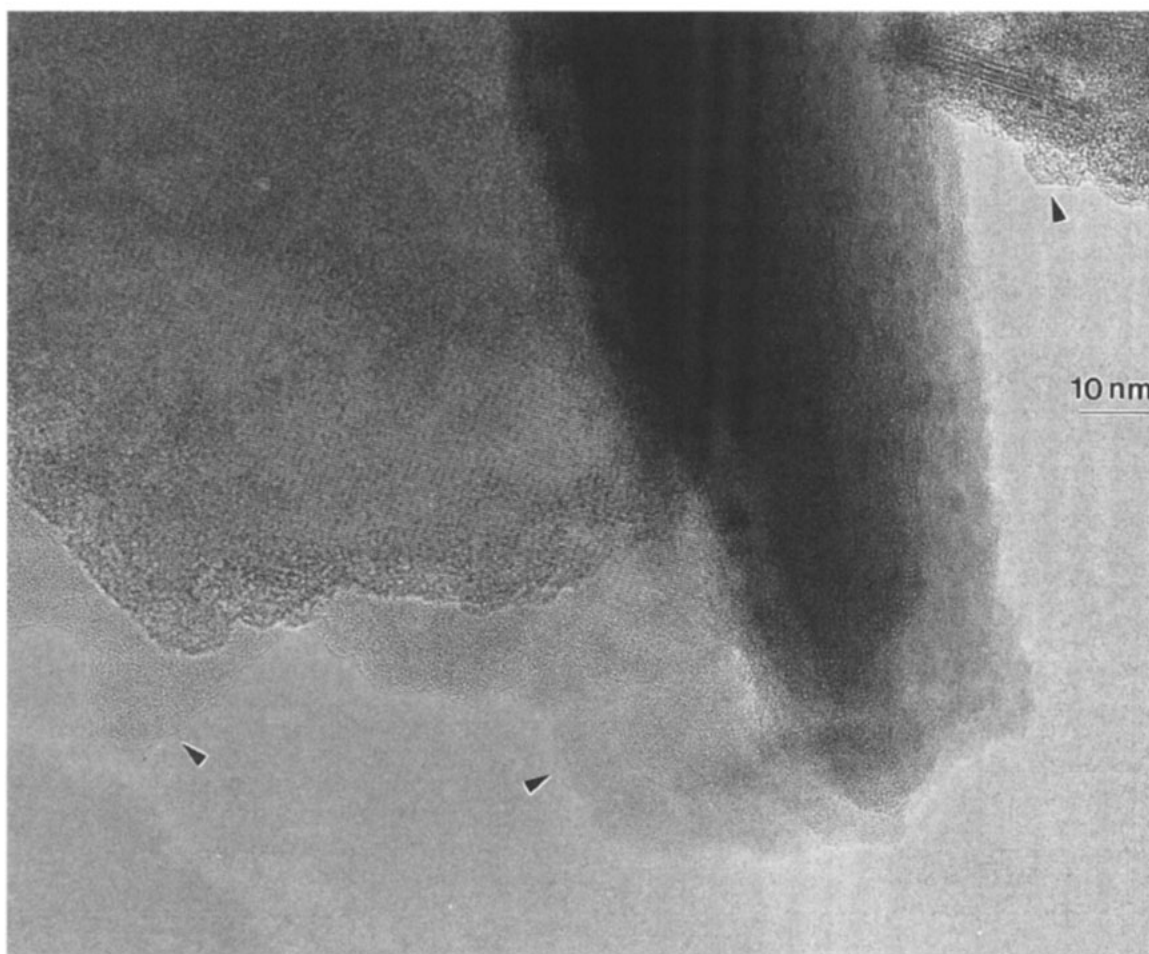


Fig. 7. High-resolution transmission electron microscope image of a Ni-treated pyrophyllite surface at a Ni sorption density of $1.44 \mu\text{mol}/\text{m}^2$. The image again shows material with a rough, scalloped, "cauliflower-like" appearance along the particle edge (compare with Fig. 5).

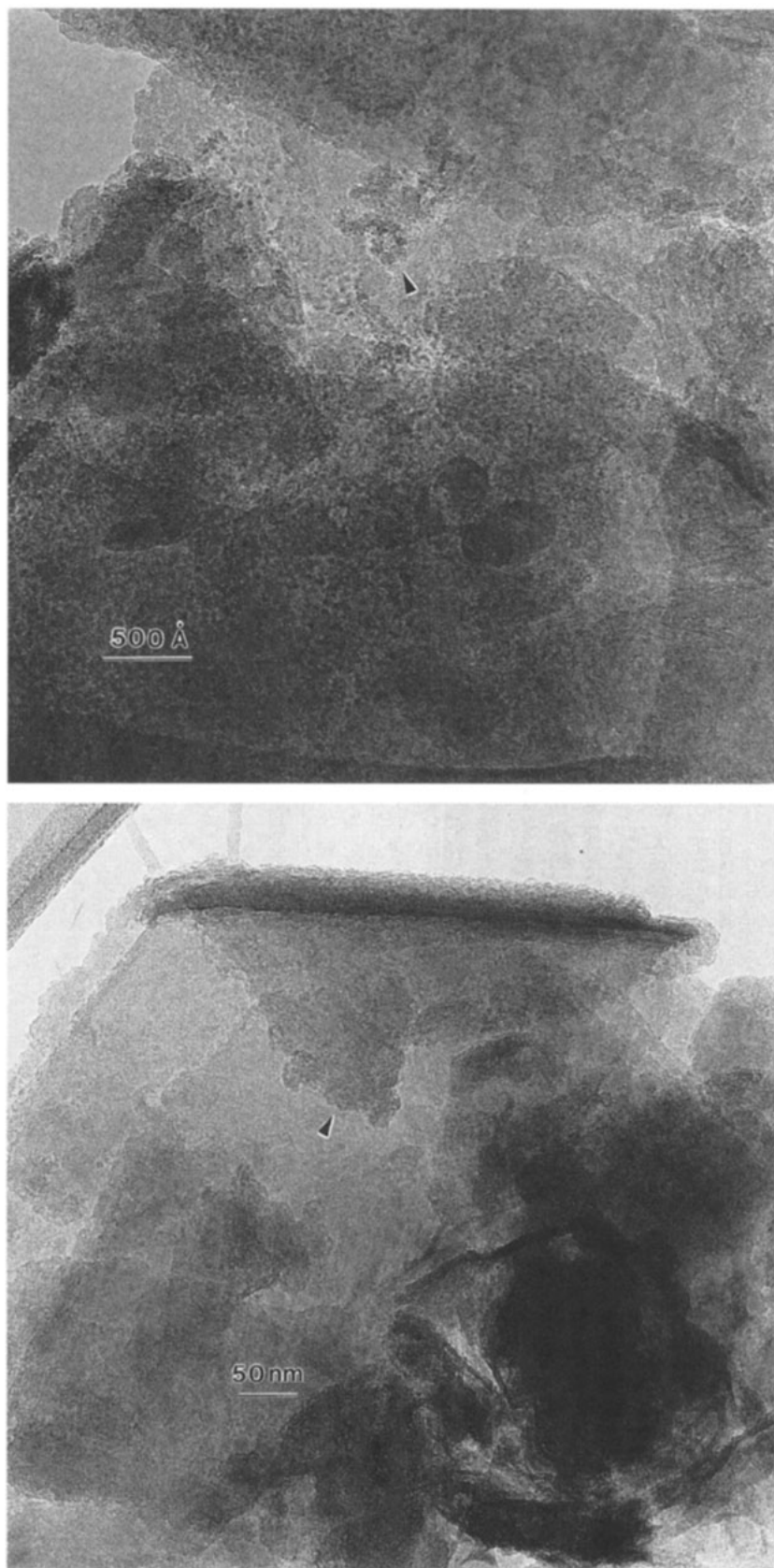


Fig. 8. Low-magnification transmission electron microscope (TEM) image of (a) a heavily Ni treated pyrophyllite particle (Ni sorption density $\approx 26.5 \mu\text{mol}/\text{m}^2$) and (b) pyrophyllite particle with much lower Ni sorption density ($0.46 \mu\text{mol}/\text{m}^2$). In both cases, suggestive changes in contrast across the particle (see arrows) indicate that surface precipitation has occurred on the top and bottom surfaces of the pyrophyllite as well as the particle edges visible in the TEM images.

apparent presence of precipitates on the top and bottom surfaces of a particle under these conditions indicates that an appreciable planar charge density must have been present in this location, and hence that there was some deviation from the "perfect" pyrophyllite stoichiometry.

We have demonstrated that Ni sorption onto pyrophyllite can result in the formation of surface precipitates. The TEM images reveal that the surface deposits are similar in samples with different Ni sorption densities, and vary only in size and spatial extent. This suggests that the structure of the surface precipitate does not depend on the Ni surface density, in agreement with the XAFS results (Scheidegger et al., 1996). Furthermore, the XAFS data indicate that the structure of the surface precipitates is similar, but not identical, to the structure of Ni(OH)₂. Observed Ni-Ni distances (≈ 3 Å) were distinctly shorter than in Ni(OH)₂ (3.09 Å). Such a bond distance indicates edge sharing of Ni and Al octahedra and the presence of mixed Ni-Al hydroxides, while the presence of a new hydrous Ni silicate phase could be excluded for other reasons (Scheidegger et al., 1996).

The existence of mixed-cation hydroxide phases has been reported in the literature (Allmann, 1970; Taylor, 1984). These compounds consist of pyroaurite-like structures in which divalent and trivalent metal ions are randomly distributed within the same octahedral hydroxide sheet. Anions such as Cl⁻, Br⁻, I⁻, NO₃⁻, OH⁻, and CO₃²⁻ can occupy the region between the hydroxide sheets. The synthesis of mixed-cation hydroxide compounds can be performed by precipitation of one cation, e.g. Al(III), as an hydroxide from solution with the pH of the suspension maintained just below the value at which the second cation hydroxide [e.g. Ni(OH)₂(s)] would precipitate (Taylor, 1984). In mixed Ni-Al hydroxides, the Ni/Al cation mole ratio can vary between 1.3 and 4.8 (Allmann, 1970; Taylor, 1984). The Ni-Ni distances in these compounds are 3.05 Å (Allmann, 1970) and therefore distinctly shorter than those in Ni(OH)₂.

The hypothesis of the formation of secondary precipitates is further supported by the findings from a dissolution study of Ni surface precipitates on pyrophyllite (Scheidegger and Sparks, 1996). Compared with the dissolution of crystalline Ni(OH)₂(s), Ni detachment from the pyrophyllite surface was slow and the data suggested the presence of secondary precipitates with a low solubility rather than the presence of Ni(OH)₂-like surface precipitates.

To conclude, we stress once again that the presence of surface precipitates on mineral surfaces has a major effect on the bioavailability, mobility, and the fate of metals in soil and water environments. Our results support the hypothesis that nucleation processes are a reason for the so called "aging effect" observed in many metal sorption experiments (Kuo and Mikkelsen, 1980; Benjamin and Leckie, 1981; Padmanabham, 1983; Lehmann and Harter, 1984; Tiller and Gerth, 1984; Davis et al., 1987; Schultz et al., 1987; Bruemmer et al., 1988; Barrow et al., 1989; Ainsworth et al., 1994). Therefore, the formation of surface precipitates should be considered in metal surface complexation modeling, in metal specia-

tion, and in risk assessments of the migration of contaminants in polluted sites.

ACKNOWLEDGMENTS

We thank R. Keren (Inst. of Soils and Water, Agricultural Research Organization, Bet Dagan, Israel) for making the pyrophyllite available, Cathy Olsen for the ICP measurements and Dan Strawn and Scott Fendorf for their careful reading of the manuscript. Electron microscopy work was performed at the National Center for Electron Microscopy, Lawrence Berkeley Laboratory, a facility funded by the Director, Office of Energy Research, Office of Basic Energy Sciences, Materials Science Division of the U.S. Department of Energy under Contract no. DE-AC03-76SF00098. We gratefully acknowledge the support of this research by the DuPont Company.

REFERENCES

- Ainsworth, C.C., J.L. Pilon, P.L. Gassmann, and W.G. van der Sluys. 1994. Cobalt, cadmium, and lead sorption to hydrous iron oxide: Residence time effect. *Soil Sci. Soc. Am. J.* 58:1615-1623.
- Allmann, R. 1970. Doppelschichtstrukturen mit brucitaehnlichen Schichten [Me(II)_{1-x}Me(III)_x(OH)₂]⁺. *Chimia* 24:99-108.
- Barrow, N.J., J. Gerth, and G.W. Bruemmer. 1989. Reaction kinetics of the adsorption and desorption of nickel, zinc, and cadmium by goethite: II. Modelling the extent and rate of reaction. *Soil Sci.* 40:437-450.
- Benjamin, M.M., and J.O. Leckie. 1981. Multi-site adsorption of Cd, Co, Zn, and Pb on amorphous iron oxyhydroxide. *J. Colloid Interface Sci.* 79:209-221.
- Bleam, W.F., and M.B. McBride. 1986. The chemistry of adsorbed Cu(II) and Mn(II) in aqueous titanium dioxide suspensions. *J. Colloid Interface Sci.* 165:269-289.
- Bruemmer, G.W., J. Gerth, and K.G. Tiller. 1988. Reaction kinetics of adsorption and desorption of nickel, zinc and cadmium by goethite. I. Adsorption and diffusion of metals. *Soil Sci.* 39:37-52.
- Charlet, L., and A. Manceau. 1993. Structure, formation, and reactivity of hydrous oxide particles: Insights from x-ray absorption spectroscopy. p. 117-164. *In* J. Buffle and H.P. van Leeuwen (ed.) *Environmental particles*. Lewis Publ., Boca Raton, FL.
- Cowan, C.E., J.M. Zachara, S.C. Smith, and C.T. Resch. 1992. Individual sorbent contributions to cadmium sorption on Ultisols of mixed mineralogy. *Soil Sci. Soc. Am. J.* 56:1084-1094.
- Davis, J.A., C.C. Fuller, and A.D. Cook. 1987. A model for trace metal sorption processes at the calcite surface: Adsorption of Cd²⁺ and subsequent solid solution formation. *Geochim. Cosmochim. Acta* 51:1477-1490.
- Farrar, H., D. Hatton, and W.F. Pickering. 1980. The affinity of metal ions for clay surfaces. *Chem. Geol.* 28:55-68.
- Fendorf, M., M. Powers, and R. Gronsky. 1995. Preparation of oxide superconductor specimens for TEM examination. *Microsc. Res. Technique* 30:167-180.
- Fendorf, S.E., and M. Fendorf. 1996. Sorption mechanisms of lanthanum on oxide minerals. *Clays Clay Miner.* 44:220-227.
- Fendorf, S.E., M. Fendorf, D.L. Sparks, and R. Gronsky. 1992a. Inhibitory mechanisms of Cr(III) oxidation by δ-MnO₂. *J. Colloid Interface Sci.* 153:37-54.
- Fendorf, S.E., G.M. Lamble, M.G. Stapleton, M.J. Kelley, and D.L. Sparks. 1994. Mechanisms of chromium(III) sorption on silica. 1. Cr(III) surface structure derived by extended X-ray absorption fine structure spectroscopy. *Environ. Sci. Technol.* 28:284-289.
- Fendorf, S.E., and D.L. Sparks. 1994. Mechanisms of Cr(II) sorption on silica. 2. Effect of reaction conditions. *Environ. Sci. Technol.* 28:290-297.
- Fendorf, S.E., D.L. Sparks, M. Fendorf, and R. Gronsky. 1992b. Surface precipitation reactions on oxide surfaces. *J. Colloid Interface Sci.* 148:295-298.
- Fendorf, S.E., R.J. Zasoski, and R.G. Burau. 1993. Competing metal ion influences on chromium(II) oxidation by birnessite. *Soil Sci. Soc. Am. J.* 57:1508-1515.
- Fletcher, P., and G. Sposito. 1989. The chemical modelling of clay/

- electrolyte interactions for montmorillonite. *Clay Clay Miner.* 24: 375-391.
- Glushko, V.P. 1972. Thermal constants of compounds. Vol. 6 (Parts 1 and 2). Academy of Sciences, USSR.
- Gurvich, L.V., I.V. Veyts, and C.B. Alcock. 1993. Thermodynamic properties of individual substances. Bigell Publ. House, New York.
- Hurlbut, C.S., Jr. 1971. Dana's manual of mineralogy. John Wiley & Sons, New York.
- Inskoop, W.P., and J. Baham. 1983. Adsorption of Cd(II) and Cu(II) by Na-montmorillonite at low surface coverage. *Soil Sci. Soc. Am. J.* 47:660-665.
- Junta, J.L., and M.F. Hochella, Jr. 1994. Manganese (II) oxidation at mineral surfaces: A microscopic and spectroscopic study. *Geochim. Cosmochim. Acta* 58:4985-4999.
- Keren R., P.R. Grossl, and D.L. Sparks. 1994. Equilibrium and kinetics of borate adsorption-desorption on pyrophyllite in aqueous suspensions. *Soil Sci. Soc. Am. J.* 58:1116-1122.
- Keren, R., and D.L. Sparks. 1994. Effect of pH and ionic strength on boron adsorption by pyrophyllite. *Soil Sci. Soc. Am. J.* 58: 1095-1100.
- Keren, R., and D.L. Sparks. 1995. The role of edge surfaces in flocculation of 2:1 clay minerals. *Soil Sci. Soc. Am. J.* 59:430-435.
- Kuo, S., and D.S. Mikkelsen. 1980. Kinetics of zinc desorption from soils. *Plant Soil* 56:355-364.
- Lehmann, R.G., and R.D. Harter. 1984. Assessment of copper-soil bond strength by desorption kinetics. *Soil Sci. Soc. Am. J.* 48: 769-772.
- McBride, M.B. 1994. Environmental chemistry of soils. Oxford Univ. Press, New York.
- McBride, M.B., A.R. Fraser, and W.J. McHardy. 1984. Cu²⁺ interaction with microcrystalline gibbsite. Evidence for oriented chemisorbed copper ions. *Clays Clay Miner.* 32:12-18.
- O'Day, P.A., G.E. Brown, Jr., and G.A. Parks. 1994a. X-ray absorption spectroscopy of cobalt(II) multinuclear surface complexes and surface precipitates on kaolinite. *J. Colloid Interface Sci.* 165: 269-289.
- O'Day, P.A., G.A. Parks, and G.E. Brown, Jr. 1994b. Molecular structure and binding sites of cobalt(II) surface complexes on kaolinite from x-ray absorption spectroscopy. *Clays Clay Miner.* 42:337-355.
- Padmanabham, M. 1983. Adsorption-desorption behavior of copper(II) at the goethite-solution interface. *Aust. J. Soil Res.* 21: 309-320.
- Peigneur, P., A. Meas, and A. Cremers. 1975. Heterogeneity of charge distribution in montmorillonite as inferred from cobalt adsorption. *Clays Clay Miner.* 23:71-75.
- Puls, R.W., and H. Bohn. 1988. Sorption of cadmium, nickel and zinc by kaolinite and montmorillonite suspensions. *Soil Sci. Soc. Am. J.* 52:1289-1292.
- Russell, J. D., V.C. Farmer, and B. Velde. 1970. Replacement of OH by OD in layer silicates, and identification of the vibrations of these groups in infra-red spectra. *Mineral. Mag.* 37:869-879.
- Scheidegger, A.M., G.M. Lamble, and D.L. Sparks. 1996. Investigation of Ni sorption on pyrophyllite: An XAFS study. *Environ. Sci. Technol.* 30:548-554.
- Scheidegger, A.M., and D.L. Sparks. 1996. Kinetics of the formation and the dissolution of Ni surface precipitates on pyrophyllite. *Chem. Geol.* (in press).
- Schindler, P.W., P. Liechti, and J.C. Westall. 1987. Adsorption of copper, cadmium and lead from aqueous solution to the kaolinite/water interface. *Neth. J. Agric. Sci.* 35:219-230.
- Schulthess, C.P., and C.P. Huang. 1990. Adsorption of heavy metals by silicon and aluminum oxide surfaces on clay minerals. *Soil Sci. Soc. Am. J.* 54:679-688.
- Schultz, M.F., M.M. Benjamin, and J.F. Ferguson. 1987. Adsorption and desorption of metals on ferrihydrite: Reversibility of the reaction and sorption properties of the regenerated solid. *Environ. Sci. Technol.* 21:863-869.
- Shock, E.L., and H.C. Helgeson. 1988. Calculation of the thermodynamic and transport properties of aqueous species at high pressures and temperatures: Correlation algorithms for ionic species and equation of state predictions to 5 kb and 1000 C. *Geochim. Cosmochim. Acta* 52:2009-2036.
- Singh, S.P.N., and S.V. Mattigold. 1992. Modeling boron adsorption on kaolinite. *Clays Clay Miner.* 40:192-205.
- Sparks, D.L. 1995. Environmental soil chemistry. Academic Press, San Diego.
- Sposito, G. 1984. The surface chemistry of soils. Oxford Univ. Press, New York.
- Sposito, G. 1986. Distinguishing adsorption from surface precipitation. *ACS Symp. Ser.* 323:217-228.
- Sverjensky, D.A. 1987. Calculations of the thermodynamic properties of aqueous species and the solubilities of minerals in supercritical electrolyte solutions. *Rev. Mineral.* 17:177-209.
- Taylor, R.M. 1984. The rapid formation of crystalline double hydroxy salts and other compounds by controlled hydrolysis. *Clay Miner.* 19:591-603.
- Tiller, K.G., J. Gerth, and G. Brümmer. 1984. The relative affinities of Cd, Ni and Zn for different soil clay fractions and goethite. *Geoderma* 34:17-35.
- Wersin, P., L. Charlet, R. Karthein, and W. Stumm. 1989. From adsorption to precipitation: Sorption of Mn²⁺ on FeCO₃(s). *Geochim. Cosmochim. Acta* 53:2787-2796.
- Wersin, P., M.F. Hochella, Jr., P. Persson, G. Redden, J.O. Leckie, and D.W. Harris. 1994. Interaction between aqueous uranium (VI) and sulfide minerals: Spectroscopic evidence for sorption and reduction. *Geochim. Cosmochim. Acta* 58:2829-2843.
- Wieland, E., and W. Stumm. 1992. Dissolution kinetics of kaolinite in acidic aqueous solutions at 25°C. *Geochim. Cosmochim. Acta* 56:3339-3355.
- Zachara, J.M., C.E. Cowan, R.L. Schmidt, and C.C. Ainsworth. 1988. Chromate adsorption by kaolinite. *Clays Clay Miner.* 36: 317-326.
- Zachara, J.M., C.T. Resch, and S.C. Smith. 1994. Influence of humic substances on Co²⁺ sorption by subsurface mineral separates and its mineralogical components. *Geochim. Cosmochim. Acta* 58:553-566.
- Zachara, J.M., S.C. Smith, J.P. McKinley, and C.T. Resch. 1993. Cadmium sorption on specimen and soil smectites in sodium and calcium electrolytes. *Soil Sci. Soc. Am. J.* 57:1491-1501.
- Zelazny, L.W., and G.N. White. 1989. The pyrophyllite-talc group. p. 527-550. In J.B. Dixon and S.B. Weed (ed.) Minerals in soil environments. 2nd ed. SSSA Book Ser. no. 1. SSSA, Madison, WI.